Biochimica et Biophysica Acta – Biomembranes 1862 (2020) 183128

Penetration of Phospholipid Membranes by Poly-L-Lysine Depends on Cholesterol and Phospholipid Composition

Amy Gorman[a,b], Khondker R. Hossain[a], Flemming Cornelius[c] and Ronald J. Clarke[a,d]

[a] *School of Chemistry, University of Sydney, Sydney, NSW 2006, Australia*

[b] *Department of Chemistry, University of York, Heslington, York, YO10 5DD, United Kingdom*

[c] *Department of Biomedicine, University of Aarhus, DK-8000 Aarhus C, Denmark*

[d] *The University of Sydney Nano Institute, Sydney, NSW 2006, Australia*

Address correspondence to Assoc. Prof. Ronald J. Clarke, School of Chemistry, University of Sydney, Sydney, NSW 2006, Australia. Tel.: 61-2-93514406; Fax: 61-2-93513329; E-mail: ronald.clarke@sydney.edu.au

Abstract

Clusters of positively-charged basic amino acid residues, particularly lysine, are known to promote the interaction of many peripheral membrane proteins with the cytoplasmic surface of the plasma membrane via electrostatic interactions. In this work, cholesterol's effects on the interaction between lysine residues and membranes have been studied. Using poly-L-lysine (PLL) and vesicles as models to mimic the interaction between lysine-rich protein domains and the plasma membrane, light scattering measurements indicated cholesterol enhanced the electrostatic interaction through indirectly affecting the negatively charged phospholipid dioleoylphosphatidylserine, DOPS. Addition of PLL to lipid vesicles containing DOPS showed an initial increase in static light scattering (SLS), attributed to binding of PLL to the vesicle surface, followed by a slower continuously declining SLS signal, which, from comparison with fluorescent dye leakage studies could be attributed to vesicle lysis. Although electrostatic interactions between PLL and the membrane were not necessary for penetration to occur, cholesterol promoted membrane disruption of negatively charged vesicles, possibly by increasing the electrostatic interactions between PLL and the membrane. In contrast, cholesterol lowered the susceptibility of uncharged vesicles (formed using dioleoylphosphatidylcholine, DOPC) to PLL penetration. This can be explained by the absence of electrostatic interactions and cholesterol's known ability to increase membrane thickness and mechanical strength. Thus, the ability of cationic peptides to penetrate membranes including cholesterol is likely to depend on the membrane's PS:PC ratio.

Keywords: carboxyfluorescein; fluorescence spectroscopy; membrane penetration; light scattering; phosphatidylserine; protein-lipid interactions

1. Introduction

It is well established that clusters of positively charged lysine residues at the N- or C-terminal of many peripheral membrane proteins promote their association with the negatively charged surface of the cytoplasmic face of the animal plasma membrane [1]. These proteins include kinases such as Src [2] and MARCKS [3, 4] as well as G proteins [5], the SH2B1β gene product [6] and the Gag protein of retroviruses such as HIV [7]. The membrane interaction of these peripheral proteins is further promoted by post-translational modifications, such as myristolyation, which attaches membrane-inserting hydrocarbon chains to the protein.

Lysine clusters are not, however, exclusive to peripheral membrane proteins. They have also been identified in some transmembrane proteins, for example, at the N-terminus of the α-subunits of the Na^+,K^+-ATPase and the gastric H^+,K^+-ATPase [8], and on the regulatory RCK domain of some K^+ channels [9]. Because these transmembrane proteins are securely embedded in their membranes by their transmembrane domains, in contrast to peripheral proteins, their lysine clusters would be unnecessary for membrane attachment. It seems more likely that any interaction of the lysine clusters of these proteins with the surrounding membrane would play a role in their ion transport mechanisms or its regulation. That the lysine residues of the Na^+,K^+-ATPase α-subunit N-terminus are performing an important function is supported by the fact that this region of the protein possesses a lysine-containing amino acid sequence, LKKE, which is conserved across all vertebrate as well as many invertebrate species [8, 10]. Trypsin digestion experiments [11-14] have shown that the LKKE motif undergoes significant movement during the protein's E2-E1 conformational transition, which switches the protein's selectivity between K^+ and Na^+, with the LKKE motif being protected from trypsin attack in the E2 state relative to E1. This change in susceptibility to trypsin attack could possibly be explained by a difference in protein folding between the E2 and E1 states, but it would also be consistent with a change in degree of membrane interaction [10, 15].

Within animal cell plasma membranes cholesterol is an essential and dominant lipid which controls the physical properties of the phospholipid bilayer. Cholesterol's ability to restrict the mobility of phospholipids by increasing hydrocarbon chain ordering and increasing membrane thickness and mechanical strength of bilayers has been well documented [16-24]. The interaction of cholesterol with membrane lipids has been extensively studied [17, 18, 21, 25-28]. However, whether cholesterol is capable of modulating the interaction of lysine-rich clusters of membrane proteins with the membrane surface is unclear. This is the topic of this study. To this aim, here we have carried out light scattering and dye leakage studies to investigate the effect of cholesterol on the possible electrostatic interaction between lysine-rich clusters and the plasma membrane, using poly-L-lysine (PLL) as a model lysine-cluster and both lipid vesicles of varying composition and purified Na^+,K^+-ATPase-containing open membrane fragments. Furthermore, the studies shed light on cholesterol's ability to alter the structural integrity of the plasma membrane with respect to penetration by lysine-rich peptides.

2. Materials and methods

2.1 Enzyme and reagents

Na^+,K^+-ATPase-containing membrane fragments from the outer medulla of pig kidney were purified as described by Klodos *et al*. [29] in pH 7.0 buffer containing 20 mM histidine, 250 mM sucrose and 0.9 mM EDTA. Each preparation was stored at -80 °C. After thawing, the preparations were aliquoted as 50 μL portions and stored at -20 °C until used. The specific ATPase activity of the preparation used at 37 °C and pH 7.4 was measured according to Ottolenghi [30] to be 1400 μmol ATP hydrolysed h^{-1} mg of $protein^{-1}$ at saturating substrate concentrations. The protein concentration was 4.0 mg mL^{-1}, determined according to the Peterson [31] modification of the Lowry [32] method using bovine serum albumin as a standard.

The origins of the other reagents used were: carboxyfluorescein (≥95%, Sigma, Castle Hill, Australia), chloroform (≥99.0%, Uvasol, Merck), cholesterol (≥99%, Sigma), EDTA (99%, Sigma), HCl (0.1 N Titrisol solution, Merck), NaCl (Suprapure, Merck, Kilsyth, Australia), poly-L-lysine (PLL) hydrochloride (MW 15,000 – 30,000 g mol^{-1}, Sigma), tris(hydroxymethyl)aminoethane (99%, Alfa Aesar, Heysham, UK) and Triton X-100 (Sigma). Dioleoylphosphatidylcholine (DOPC) and dioleoylphosphatidylserine sodium salt (DOPS) were obtained from Avanti Polar lipids (Alabaster, AL, USA).

Based on the degree of polymerisation of the PLL used, to convert the concentration of PLL in μg mL^{-1} to μM of lysine (i.e. monomer) units one needs to multiply by a factor of 6.1.

2.2 Vesicle preparation

Unilamellar lipid vesicles were synthesised by first preparing separate 3 mM stock solutions of cholesterol, DOPS and DOPC dissolved in chloroform. A chloroform density of 1.48 g mL^{-1} was used to prepare the stock solutions by weight. Accurate volumes of the 3 mM lipid stock solutions were mixed in the appropriate cholesterol, DOPS and DOPC volume ratios to obtain the final desired mol% solution. Depending on the amount of vesicle preparation required for an experiment, the total solution volume varied in the range 0.5 – 5 mL. Chloroform was extracted from the solutions *in vacuo* at 60°C and 474 mbar using a rotary evaporator at a fast rotation speed. Once no traces of chloroform could be seen, the pressure was reduced to 0 mbar for a further 20 min to ensure complete chloroform removal. The dried lipid film was hydrated with the same volume of buffer (30 mM Tris, 150 mM NaCl, 1 mM EDTA, pH 7.2) as used for the initial chloroform solution in order to regain a final total lipid concentration of 3 mM. The hydrated lipid film was sonicated for 20 min to ensure total lipid resuspension and extruded 11 times through a 0.1 μm Nucleopore polycarbonate membrane

using an Avanti Mini-Extruder (Alabaster, AL, USA) at room temperature to obtain a unilamellar vesicle suspension.

2.3.1 Static Light Scattering of Vesicles

Static light scattering (SLS) measurements of vesicles were recorded using an RF-5301 PC spectrofluorophotometer (Shimadzu, Tokyo, Japan) with 1 cm path length quartz semi-microcuvettes and the temperature maintained at 24 °C *via* a circulating water bath. The wavelengths of both the incident and the observed Rayleigh scattered radiation were 824 nm, as used by Nguyen *et al*. [10]. This wavelength showed the greatest relative increase in SLS upon addition of PLL to vesicles and corresponds to a high intensity line in the spectrum of the xenon arc lamp of the instrument. The bandwidths were 5 nm and the SLS was detected at 90° to the incident light. Before adding vesicles to the cuvette, the SLS signal was allowed to stabilise (typically 3-5 mins) with buffer alone (30 mM Tris, 150 mM NaCl, 1 mM EDTA, pH 7.2) in the cuvette. After adding vesicles, the SLS signal was again left to stabilise (typically 5-7 mins). For each experiment, prior to PLL addition, the same initial SLS signal level was used, but depending on the vesicle composition, different vesicle volumes (15-150 μL), and therefore total lipid concentrations (45-450 μM of combined DOPS, DOPC and cholesterol), were needed to achieve this level. The total volume of buffer and vesicles, prior to PLL addition, was 1 mL. Finally, poly-L-lysine (PLL) (0.5 – 9 μL, 0.1 μg μL^{-1} or 0.3 – 5 μL, 1 μg μL^{-1}) was added to the cuvette. As small volumes of PLL solution were added to the cuvette (<10 μL), all calculations of PLL concentrations were based on a final volume of 1 mL.

2.3.2 Static Light Scattering of Na^+,K^+-ATPase Membrane Fragments

SLS measurements of Na^+,K^+-ATPase membrane fragments were recorded under the same conditions as those of vesicle measurements, with the exception of a very slightly longer

wavelength of the incident and the scattered light of 826 nm, as this wavelength produced the greatest SLS signal difference upon PLL addition to Na^+,K^+-ATPase membrane fragments [10]. Buffer (990 μL, 30 mM Tris, 150 mM NaCl, 1 mM EDTA, pH 7.2) was added to the cuvette, the SLS signal was allowed to stabilise (typically 2-3 mins), after which Na^+,K^+-ATPase membrane fragments (10 μL, 4.0 mg mL^{-1}) were added. The suspension of Na^+,K^+-ATPase membrane fragments was again left to stabilise (typically 2-3 mins) to give a light intensity level similar to that used for the vesicle measurements. PLL was then introduced to the cuvette (3 μL, 50 μg μL^{-1}). All SLS control experiments were performed using the same instrument settings as described for SLS experiments with either vesicles or Na^+,K^+-ATPase membrane fragments. Control experiments in which PLL (3 μL, 50 μg μL^{-1}) was added to a cuvette containing buffer (1000 μL, 30 mM Tris, 150 mM NaCl, 1 mM EDTA, pH 7.2) showed no increase in SLS above the buffer baseline, confirming that PLL alone did not perturb the SLS.

2.4 Dynamic Light Scattering

Dynamic light scattering (DLS) experiments with vesicles were carried out using a Zetasizer Nano series (Malvern Instruments, Malvern, UK) with a helium neon laser at a wavelength of 632.8 nm. A 1 cm path length quartz semi-microcuvette was rinsed with deionized water and ethanol before being sonicated for 30 min in 2 M HCl. Following sonication, the cuvette was again rinsed with ethanol and dried with nitrogen. This intensive cleaning process of the cuvette ensured no small particulates on the nm scale interfered with the DLS measurements. Buffer (980 μL, 30 mM Tris, 150 mM NaCl, 1 mM EDTA, pH 7.2) was added to the cuvette, followed by the addition of vesicles (20 μL). PLL (0.2-8 μL, 0.1 μg μL^{-1}) was continuously titrated into the cuvette to obtain the desired final PLL concentrations. The final solution was mixed thoroughly before DLS measurements were taken to prevent unwanted aggregate

sedimentation. Measurements were taken at 24 °C in triplicate at a backscatter angle of 173° and averaged to obtain the final average particle diameter. As the volume of PLL titrated into the cuvette was below 10 μL, the concentration of PLL in the cuvette was calculated based on a total volume of 1 mL. Control experiments in which PLL (10 μL, 0.1 μg μL^{-1}) was added to a cuvette in the absence of vesicles (1000 μL, 30 mM Tris, 150 mM NaCl, 1 mM EDTA, pH 7.2) showed no observable DLS signal in the size range of the vesicles. Autocorrelation analysis of the time-dependent fluctuations in the light scattering signal [33] yielded the three-dimensional diffusion coefficient of the vesicles, which, based on the assumption that the vesicles are spherical, could be converted via the Stokes-Einstein equation into an average vesicle hydrodynamic diameter, Z-avg. This analysis was carried out via software provided with the instrument.

2.5 Carboxyfluorescein Encapsulation within Vesicles

Unilamellar lipid vesicles were prepared using the same procedure as described in Section 2.2 with lipid stock solutions of 30 mM and hydrated with a solution of carboxyfluorescein (CF) in buffer (1 mL, 200 mM carboxyfluorescein in 30 mM Tris, 150 mM NaCl, 1 mM EDTA, pH 7.2). Prior to hydration of the lipid film, the pH of the carboxyfluorescein solution was adjusted to pH 7.4 with 1 M NaOH to ensure complete solubilisation of the dye. This results in a translucent dark brown solution. Carboxyfluorescein-containing vesicles were purified by size exclusion chromatography using a Sephadex G-25 PD-10 column in buffer (30 mM Tris, 150 mM NaCl, 1 mM EDTA, pH 7.4). Fractions containing carboxyfluorescein-encapsulated vesicles were distinguished by observing an increase in fluorescence intensity upon addition of Triton-X (50 μL, 2% v/v) to individual fractions (10 μL in 990 μL 30 mM Tris, 150 mM NaCl, 1 mM EDTA, pH 7.4) (See 2.6 for fluorescence measurement details). Fractions that contained carboxyfluorescein vesicles had a

cloudy appearance in comparison to the translucent solution of free carboxyfluorescein. All fractions containing carboxyfluorescein-encapsulated vesicles were combined and vortexed prior to PLL titration. Fluorescence measurements of CF-encapsulated vesicles between 12 and 24 hours after initial vesicle preparation displayed significantly higher fluorescence intensities than vesicles prepared within 12 hours of preparation. This indicated that dye begins to leak out of the vesicles after 12 hours. Thus, experiments were conducted within 12 hours of vesicle preparation.

2.6 Measurement of Penetration of Carboxyfluorescein-Containing Vesicles by PLL

Fluorescence emission spectra were recorded over the emission wavelength range 400-700 nm using an RF-5301 PC spectrofluorophotometer (Shimadzu, Tokyo, Japan) with 1 cm path length quartz microcuvettes and an excitation wavelength of 490 nm. The bandwidths were 5 nm for both the excitation and emission monochromators. The temperature of the solution in the cuvette was maintained at 24 °C *via* a circulating water bath. A solution of buffer (990 μL, 30 mM Tris, 150 mM NaCl, 1 mM EDTA, pH 7.4) and carboxyfluorescein-containing vesicles (10 μL) were added to the cuvette. PLL was added to the solution (50 μL, 1 μg μL^{-1}) followed by Triton X-100 (50 μL, 2% v/v) to completely lyse the vesicles. Fluorescence intensity change upon PLL addition to carboxyfluorescein-loaded vesicles was expressed as a percentage of the maximum carboxyfluorescein intensity obtained upon complete vesicle lysis by addition of detergent Triton X-100, as described by equation 1.

$$\Delta F(\%) = \frac{F^{PLL} - F^{V}}{F^{TX} - F^{V}} \times 100 \quad (1)$$

The individual terms in the equation represent the maximum fluorescence intensity at an emission wavelength of 516 nm upon addition of carboxyfluorescein vesicles (F^{V}), with

subsequent addition of PLL (F^{PLL}) and Triton X-100 (F^{TX}). The calculation was carried using the emission wavelength of 516 nm because this corresponds to the wavelength of maximum fluorescence emission of carboxyfluorescein.

To test the effect of PLL on carboxyfluorescein fluorescence, control experiments were performed in the absence of vesicles. These measurements were recorded under the same conditions as those used to investigate the penetration of vesicles by PLL. A solution of carboxyfluorescein (1 mL, 200 nM carboxyfluorescein in 30 mM Tris, 150 mM NaCl, 1 mM EDTA, pH 7.2) was added to the cuvette and PLL was continually titrated to the solution (1, 2, 10, 20, 50, 100 μL, 1 μg μL^{-1}) and an emission spectrum recorded.

3. Results

3.1 Effect of the interaction of poly-L-lysine with vesicles and Na^+,K^+-ATPase membrane fragments on membrane aggregation

Lipid analysis of native Na^+,K^+-ATPase membrane fragments showed they contained 36 mol% cholesterol and 13 mol% DOPS [34, 35]. However, DOPS is known to be concentrated in the cytoplasmic leaflet [36, 37], with flipping of DOPS to the extracellular leaflet being shown to be a signal for cell apoptosis [38, 39]. Assuming all the DOPS is located on the cytoplasmic side of the membrane, the expected level of DOPS in the cytoplasmic leaflet would be approximately 30%. Thus, for the formation of vesicles, a composition of 40% cholesterol: 30% DOPS: 30% DOPC was chosen to approximate the physiological environment, where DOPC is a zwitterionic phospholipid of the plasma membrane used to make up the remaining composition of the vesicle.

In order to compare the effect of cholesterol, vesicles with the same DOPS content as that used to represent physiological levels (i.e. 30% DOPS) but in the absence of cholesterol, 30% DOPS: 70% DOPC, was also tested. Keeping this phospholipid ratio (3: 7 DOPS: DOPC)

constant and introducing 40% cholesterol results in a composition of 40% cholesterol: 18% DOPS: 42% DOPC, which was also tested to further investigate cholesterol's effect on the relative ratios of negatively charged phospholipids. A final vesicle composition of 18% DOPS: 82% DOPC was tested to be able to observe effects on vesicles of both 30% and 18% DOPS with and without 40% cholesterol. In order to compare the increase in SLS upon PLL addition to the various vesicle compositions, the same initial SLS intensities needed to be achieved. However, different lipid concentrations of the various vesicle compositions were required to achieve the desired initial SLS range. The reason for this is unclear at this stage, but it could be related to differences in the refractive indices of vesicles of varying composition. To account for variation in lipid concentration, a ratio of PLL to total vesicle lipid concentration, (45-450 μM of combined DOPS, DOPC and cholesterol), was used, R_P (see eq. 2).

$$R_P = \frac{\text{PLL } (\mu\text{M of monomer units})}{\text{Vesicle Lipid } (\mu\text{M})} \tag{2}$$

PLL addition to anionic vesicles containing DOPS caused significant SLS increases (Figure 1) due to positively charged PLL binding to negatively charged membrane surface phospholipids, thus neutralising electrostatic repulsion between vesicles. This allowed vesicle aggregation via van der Waals forces, with more light being scattered by larger aggregates. Hence, increased light scattering was correlated to greater electrostatic interactions. Greater SLS increases were observed for vesicles containing 18% DOPS than 30%. In contrast, PLL had no effect on the SLS of net neutral vesicles comprised of DOPC with or without

cholesterol. These results agree with previous reports that negatively charged phospholipids promote electrostatic interactions with PLL [10, 40].

Figure 1: Effect of PLL addition on the static light scattering (SLS) of lipid vesicles. The

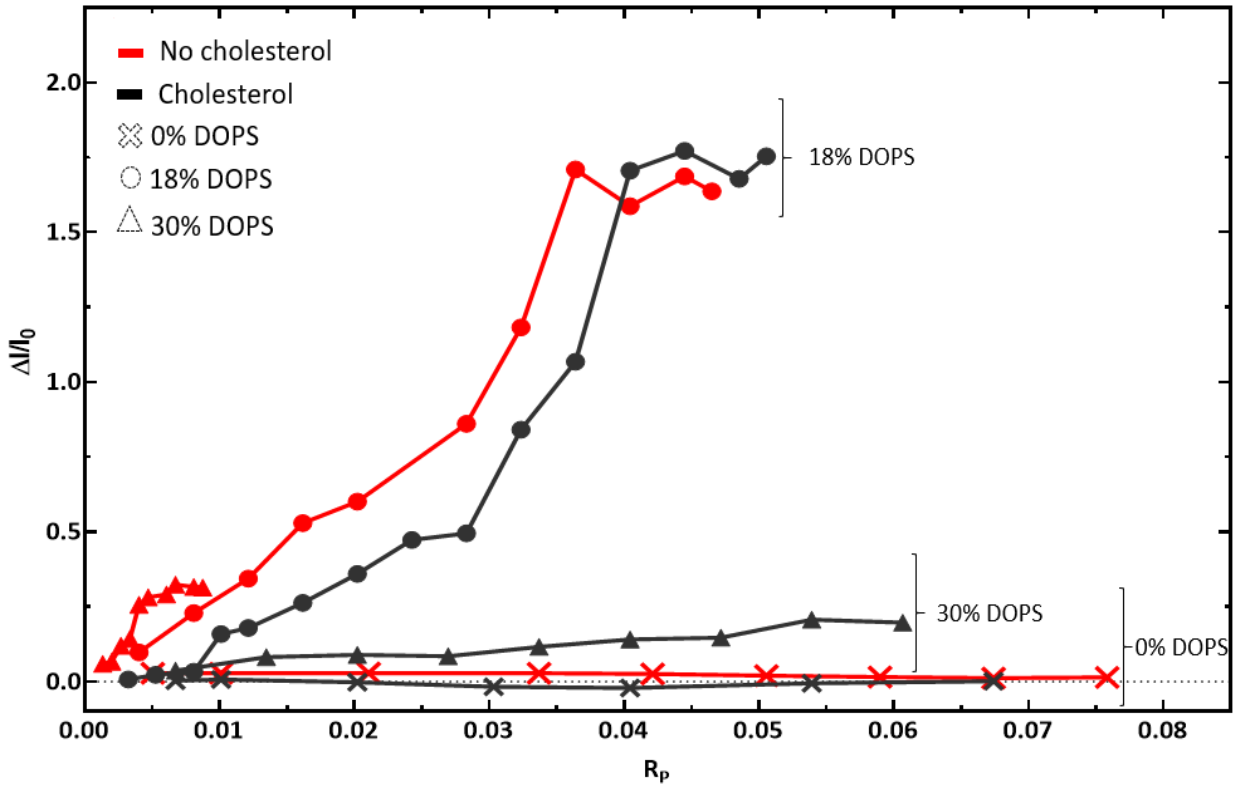

vesicles (45-450 μM total lipid) included of 0% (red) or 40% cholesterol (black). Crosses, circles and triangles represent vesicles containing 0%, 18% and 30% DOPS, respectively. The remaining percentage of lipid was DOPC. SLS is represented as the change in SLS, ΔI, upon PLL addition relative to SLS prior to PLL addition, I_0. PLL concentration is given as a ratio, R_P, between PLL in μM of monomer units, and total vesicle lipid concentration in μM. Measurements were performed at incident and observed scattered wavelengths of 824 nm with bandwidths of 5 nm for both in 30 mM Tris, 150 mM NaCl, 1 mM EDTA, pH 7.2 at 24 °C. Each point corresponds to an individual measurement on a separate vesicle sample.

Addition of PLL to vesicles including DOPS at PLL concentrations above that of the data points in Figure 1 caused a biphasic light-scattering response (Figure 2), where the SLS

signal initially increased but then continuously declined over time. The PLL concentrations that were required to induce this biphasic SLS change for different vesicle compositions are termed R_P thresholds. The maximum SLS intensity (i.e. before the SLS decline) of biphasic responses at [PLL} > R_P thresholds was always higher than the maximum SLS intensity of monophasic increases at [PLL] < R_P thresholds. Once the R_P threshold was reached, any further increase in the PLL concentration added caused no further change in the observed time course of the light scattering response, i.e. the observed traces were always biphasic with the same maximum SLS intensity.

Other studies have shown that PLL interaction with the membrane induces vesicle penetration [41, 42]. As the maximum SLS intensity achieved by the initial SLS increase of biphasic responses was constant and always greater than that of monophasic SLS increases, this is consistent with the initial SLS increase of the biphasic responses being due to the onset of vesicle lysis. The breakup of closed vesicles into membrane fragments would be expected to increase light scattering. Furthermore, the results are consistent with instantaneous lysis produced by a critical PLL concentration (hence the term R_p *threshold*). No SLS decrease was observed for vesicles lacking DOPS over the studied range of $R_P < 0.08$.

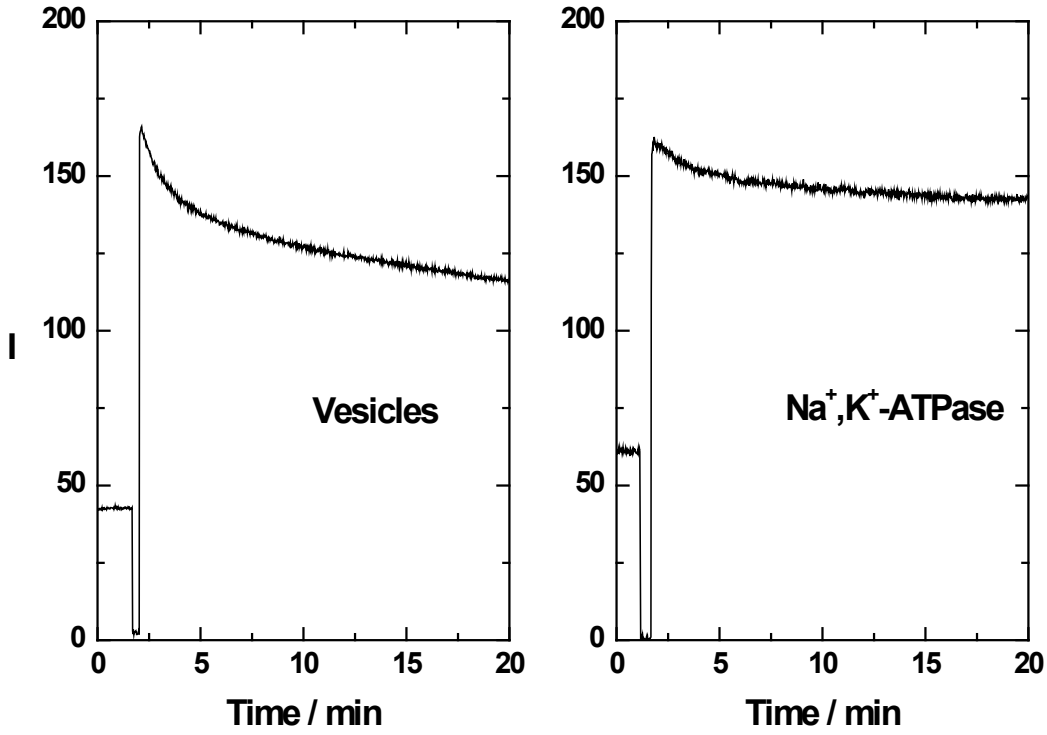

Figure 2: Biphasic SLS responses of vesicles (left) and Na^+,K^+-ATPase-containing membrane fragments (right) to the addition of PLL. In both cases PLL was added to the vesicle or membrane fragment suspension after approximately 2 minutes. Measurements were performed at incident and observed scattered wavelengths of 824 nm (vesicles) or 826 nm (Na^+,K^+-ATPase membrane fragments) with bandwidths of 5 nm in a buffer containing 30 mM Tris, 150 mM NaCl, 1 mM EDTA, pH 7.2 at 24 °C. The concentrations of PLL added were 1.5 μg mL^{-1} (9 μM of lysine residues) for the vesicle measurement and 150 μg mL^{-1} (900 μM of lysine residues) for the Na^+,K^+-ATPase measurement. The vesicles were composed of 15% DOPS and 85% DOPC, with a total lipid concentration in the cuvette of 150 μM. The Na^+,K^+-ATPase concentration in the cuvette was 40 μg mL^{-1}.

The possibility of the SLS drop being due to sedimentation was excluded because solution mixing failed to increase the SLS signal again. Osmotically induced changes in vesicle

size could also be excluded because open Na^+,K^+-ATPase-containing membrane fragments also displayed a biphasic SLS response, although much higher concentrations of PLL were required to observe the biphasic SLS signal in the case of Na^+,K^+-ATPase-containing membrane fragments than in the case of lipid vesicles (Figure 2). The biphasic behaviour was only observed for the Na^+,K^+-ATPase membrane fragments once the PLL concentration exceeded 55 μM of lysine residues. Taken together, the results obtained with both lipid vesicles and Na^+,K^+-ATPase membrane fragments suggest that above a certain threshold concentration PLL is capable of disrupting the membrane. The fact that the threshold concentration is higher for Na^+,K^+-ATPase membrane fragments than for lipid vesicles is consistent with the suggestion [10] that the Na^+,K^+-ATPase membrane fragments are more resistant, perhaps due to their high protein content.

3.2 Effect of the interaction of poly-L-lysine with vesicles on average vesicle diameter

Cationic peptides binding to negatively charged phospholipid membrane mixtures have been extensively studied and shown to form large aggregates [41, 42]. With the biphasic SLS response only being observed for vesicles containing DOPS, this suggested the presence of an electrostatic interaction. To further investigate the interaction between vesicles and PLL, DLS studies were undertaken to estimate the average vesicle diameter, Z-avg.

As seen in Figure 3, PLL addition to 0% DOPS vesicles failed to significantly increase Z-avg over the studied range. An increase in Z-avg was only observed for vesicles containing the negatively charged DOPS in addition to neutral DOPC. This confirmed that electrostatic interactions between PLL and negatively charged phospholipids induced effective vesicle neutralisation and aggregation. The increase in Z-avg was found to be considerably greater when cholesterol, as well as DOPS, were included in the vesicle composition (Figure 3). This appears, at first sight, to be inconsistent with the SLS measurements (Figure 1), which showed

higher levels of PLL-induced light scattering for vesicles without cholesterol across most of the PLL concentration range. This apparent discrepancy in the DLS and SLS results will be discussed later in more detail in the Discussion.

When the DOPS composition is increased from 18 to 30%, the DLS studies indicate a significant drop in Z-avg. This is consistent with the SLS measurements (Figure 1), which also show a significant drop in the light scattering change after PLL addition. Presumably the increase in negative surface charge density on going from 18 to 30% makes it more difficult for PLL to effectively screen the vesicle surface charge, reduce electrostatic repulsion between vesicle surfaces and allow aggregation.

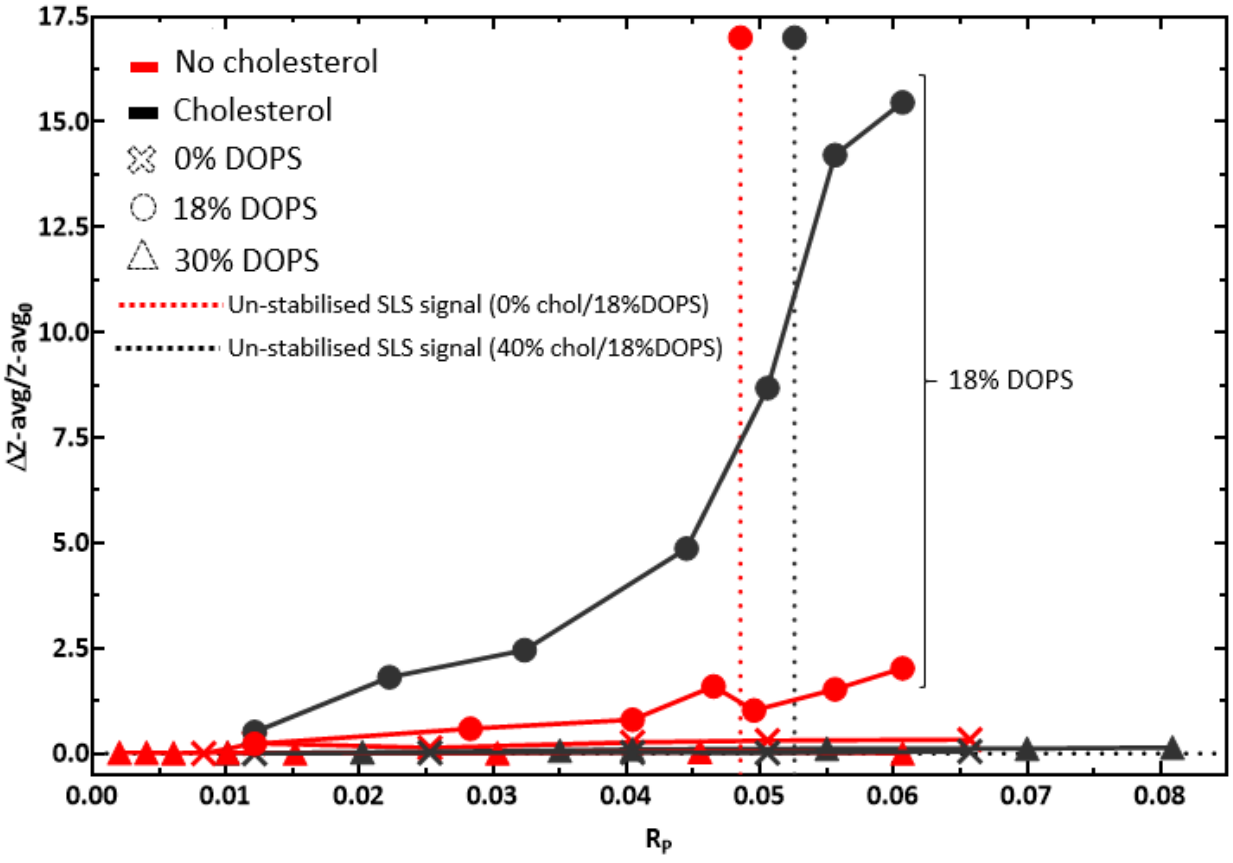

Figure 3: Effect of PLL on relative average particle diameter of vesicles (60 μM total lipid) including 0% (red) or 40% cholesterol (black). Crosses, circles and triangles represent vesicles containing 0%, 18% and 30% DOPS, respectively. In each case the remaining percentage of lipid was DOPC. Particle diameter is given in terms of the change in average particle diameter

upon PLL addition, ΔZ-avg, relative to initial average particle diameter of vesicles, Z-avg$_0$. Measurements were taken immediately after PLL addition and mixing. Z-avg and Z-avg$_0$ were calculated by size distribution by intensity and averaged over three repeated measurements. The initial average particle diameter, Z-avg$_0$, for all vesicle compositions was between 109 nm to 125 nm. PLL concentration is given as a ratio, R_P, between PLL in μM of monomer units, and total vesicle lipid concentration in μM. Measurements were performed in a buffer of 30 mM Tris, 150 mM NaCl, 1 mM EDTA, pH 7.2 and 24 °C. The dotted lines represent SLS R_P thresholds, i.e., concentrations at which biphasic SLS starts to occur. Each point corresponds to an average of three measurements.

For 18% DOPS vesicles lacking cholesterol, a decrease in Z-avg was seen at R_P ~0.05. This was a similar R_P value to the SLS R_P threshold. Despite increased PLL concentrations continuously increasing Z-avg for 40% cholesterol/18% DOPS vesicles, a small intensity peak at 355 nm appeared at R_P ~0.05 (Figure 4A), slightly below the vesicles R_P threshold at 0.053 (Figure 1). No other PLL addition to vesicles elicited the formation of a secondary peak. After 30 minutes the secondary peak disappeared, and the peak at 1245 nm shifted to 1436 nm (Figure 4B). This data supported R_P thresholds being indicative of smaller particle formation and vesicle lysis. Importantly, the Z-avg of the particles formed as a consequence of PLL titration (355 nm) remained larger than the initial vesicle size prior to PLL addition (125 nm), indicating the particles generated by addition of PLL in a concentration close to the R_P threshold originated from membrane deformation of the large vesicle aggregates and not randomly dispersed vesicles undergoing reversible aggregation.

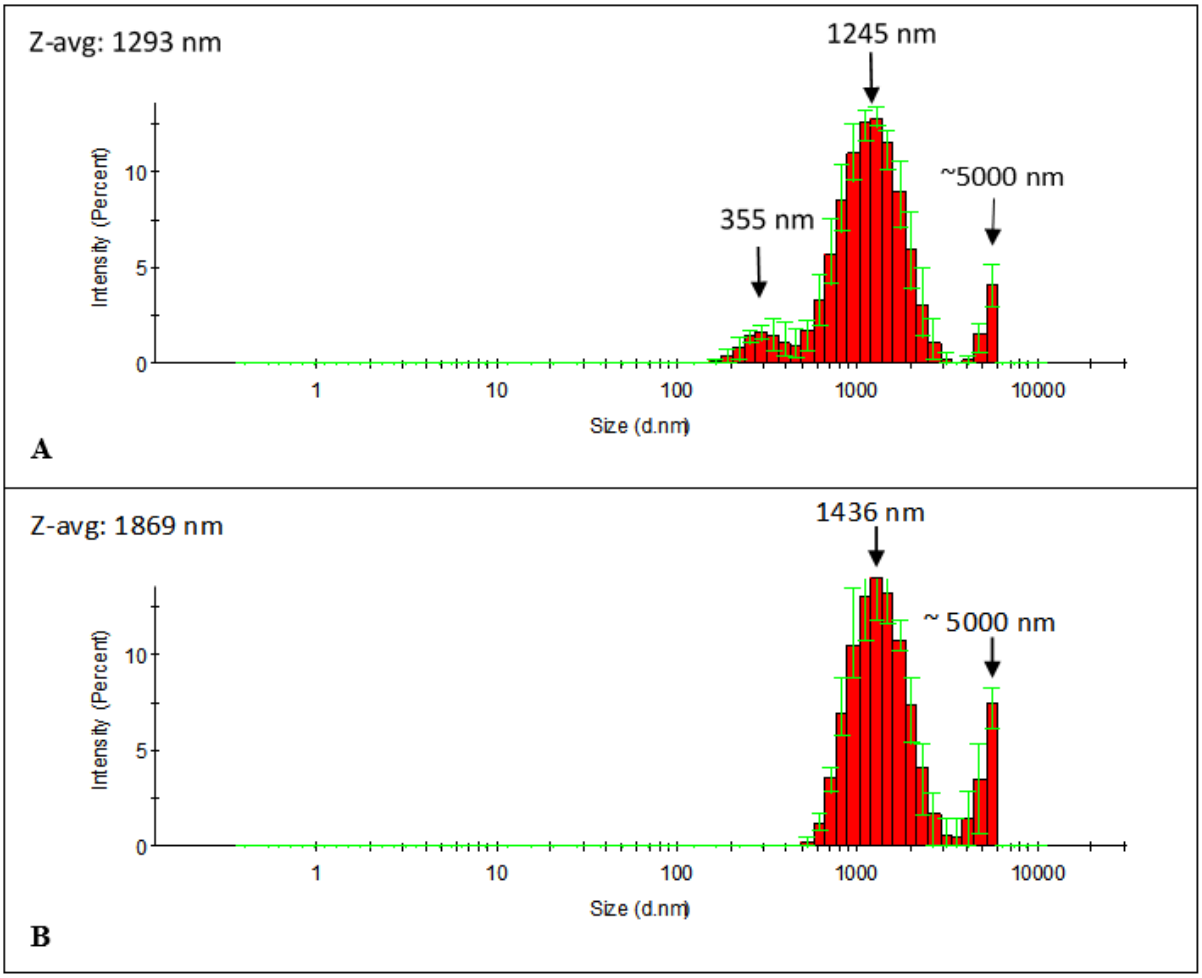

Figure 4: Averaged size distribution by intensity plot of the average particle diameter (nm) of vesicles comprised of 40% cholesterol 18% DOPS and 42% DOPC (60 μM total lipid) in a buffer of 30 mM Tris, 150mM NaCl, 1 mM EDTA, pH 7.2) immediately (A) and 30 minutes (B) after addition of PLL (3.03 μM of monomer units, R_P ~0.05) with thorough mixing prior to the DLS measurements at 24 °C. Average particle diameter, Z-avg, and peak maxima labelled. Error bars represent standard deviation of three repeated measurements.

3.3 PLL penetration of vesicle membranes

In order to enhance our understanding of the effect of PLL on vesicle aggregation and possible lysis, carboxyfluorescein experiments were conducted. Previous studies have shown that PLL membrane disruption of negatively charged phospholipid vesicles induces fluorescent

dye leakage [40]. Therefore, CF loaded vesicles were used to investigate cholesterol's effect upon PLL penetration. Encapsulated in the vesicle, CF was quenched and produced a low intensity fluorescence, consistent with previous studies [43]. Upon CF release from the vesicle to the surrounding environment, the dye is no longer quenched, and fluorescence intensity increases. Any disruption caused to vesicle membranes by PLL were indicated by perturbations in CF fluorescence intensity.

PLL addition to 100% DOPC vesicles resulted in the greatest membrane disruption (Figure 5) compared to vesicles including cholesterol and/or DOPS. Considering vesicles lacking DOPS, 100% DOPC vesicles suffered more membrane disruption by PLL than cholesterol/DOPC vesicles. This suggested cholesterol's ability to increase the ordering of the phospholipid tails, to increase membrane thickness, and provide increased mechanical stability may have prevented complete vesicle lysis by PLL, unlike vesicles of 100% DOPC (Figure 5) [21, 22]. Separate addition of either cholesterol or DOPS to DOPC vesicles resulted in decreased disruption of the vesicle membrane, demonstrating cholesterol's and DOPS' ability to provide structural integrity to the membrane against PLL penetration, with little difference shown between 18% or 30% DOPS. However, introduction of 18% or 30% DOPS induced less penetration of the membrane by PLL than 40% cholesterol, demonstrating the comparative ability of DOPS and cholesterol to increase membrane rigidity [21, 22, 44].

Interestingly the combination of cholesterol/DOPS/DOPC in the vesicle membrane similarly reduced PLL's ability to penetrate the membrane compared to 100% DOPC membranes but failed to strengthen the membrane more than vesicles including DOPC and either cholesterol or DOPS alone. This finding suggests that the combination of cholesterol and DOPS results in cholesterol condensing the negatively charged phospholipids. This would increase the negative charge density of the membrane, resulting in increased electrostatic

attraction for PLL, greater membrane disruption and CF leakage, although providing greater structural integrity to the membrane than 100% DOPC vesicles.

Significantly, PLL was able to penetrate vesicles containing cholesterol with 18% DOPS to a greater extent than 30% DOPS. It is unclear why lower levels of penetration were seen for vesicles of higher DOPS content as it would be expected that greater DOPS contribution should elicit a greater electrostatic interaction with PLL, and hence greater penetration. It could be that cholesterol's ability to increase the mechanical stability of the membrane could also have a DOPS concentration dependence, with more DOPS eliciting stronger membranes. It has been shown that cholesterol prefers to associate with DOPS over DOPC to form lipid domains of increased membrane thickness and mechanical strength [26, 45]. Therefore, it can be speculated that cholesterol may provide greater structural stability to vesicles with an increased ratio of DOPS: DOPC.

Intriguingly, although PLL addition to CF-loaded vesicles resulted in increased fluorescence intensity (Figure 5), continuous PLL addition to CF in solution resulted in CF quenching (Figure 6). These observations demonstrate that PLL is unavailable to quench free

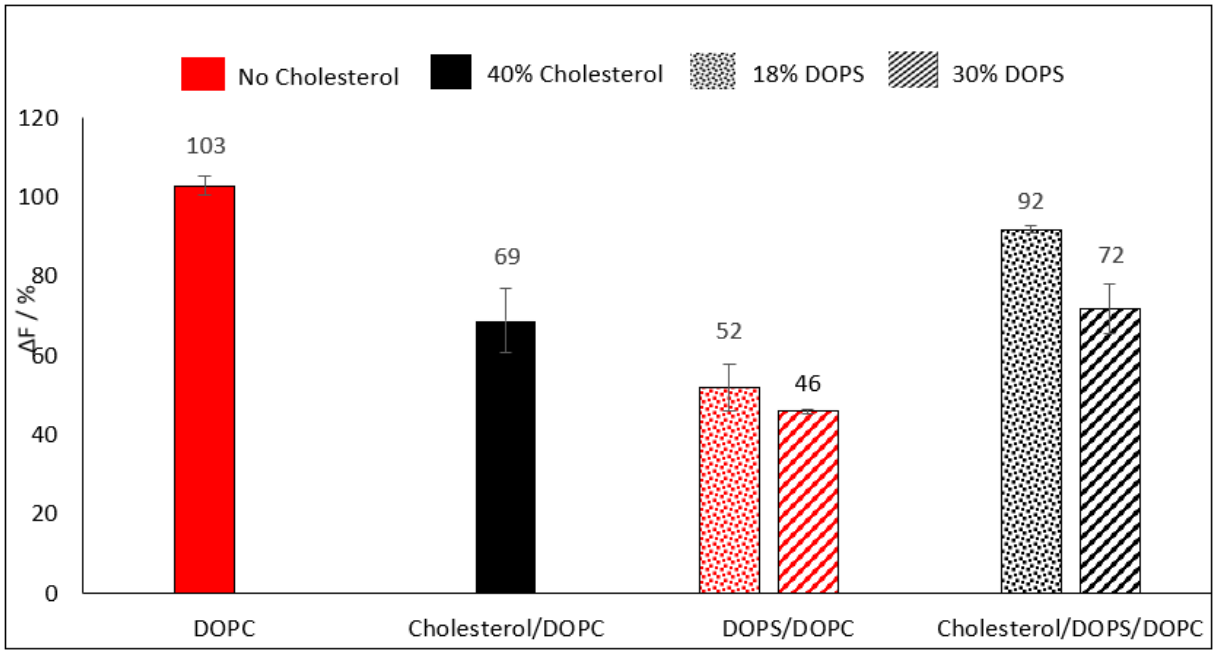

CF in solution when in the presence of a lipid membrane. This suggests that PLL is irreversibly bound to the membrane following penetration.

Figure 5: Percentage change in fluorescence intensity at an emission wavelength of 516 nm upon PLL addition (303 µM) to CF vesicles (10 µL in 990 µL, 30 mM Tris, 150 mM NaCl, 1 mM EDTA, pH 7.2). 100% intensity change represents relative fluorescence intensity change upon complete vesicle lysis by addition of Triton X-100 (50 µL, 2%). The results were averaged over three repeated measurements. Measurements were taken at an excitation wavelength of 490 nm with bandwidths of 5 nm at 24 °C.

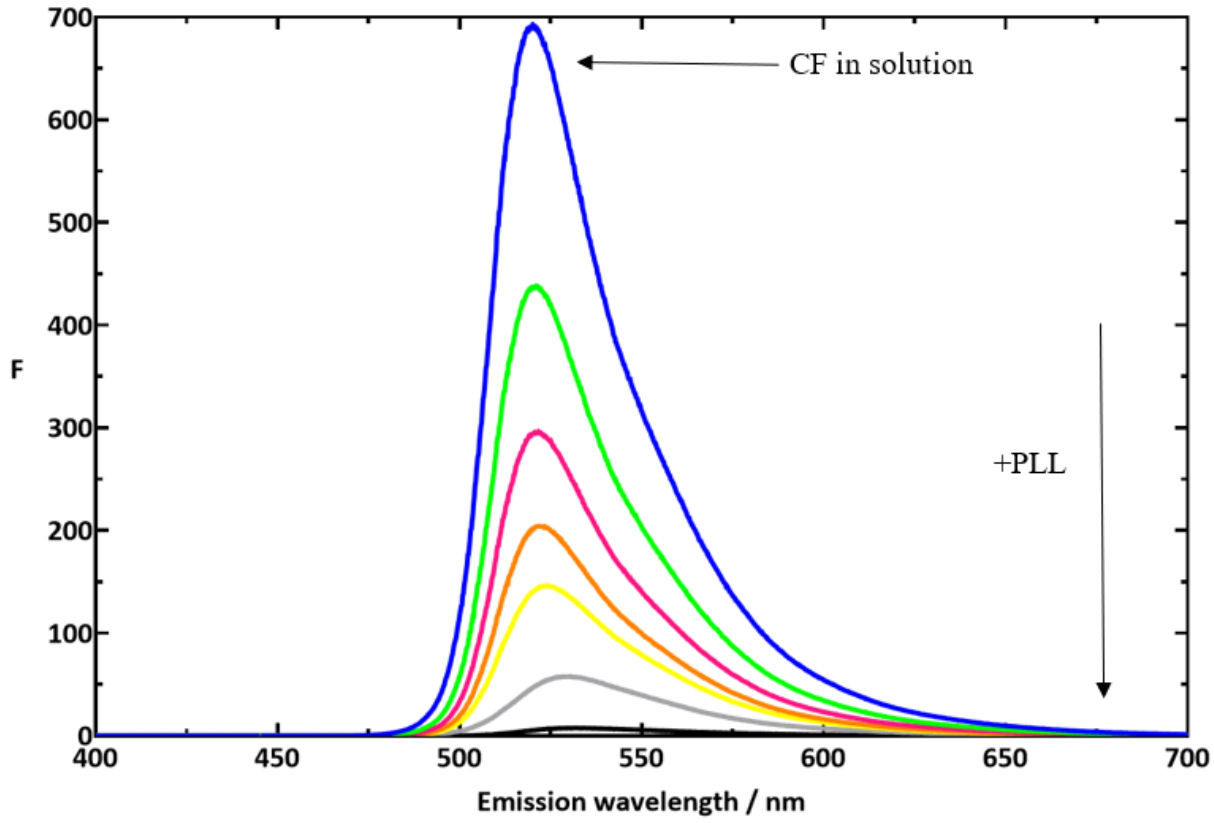

Figure 6: Emission spectra at an excitation wavelength of 490 nm with excitation and emission bandwidths of 5 nm at 24 °C. The blue line is free CF in buffer (1 mL, 200 nM CF in 30 mM Tris, 150 mM NaCl, 1 mM EDTA, pH 7.2). The descending lines are subsequent addition of

PLL (1 μg μL^{-1}) in total PLL volumes 1 μL (green), 2 μL (pink), 10 μL (orange), 20 μL (yellow), 50 μL (grey) and 100 μL (black).

4. Discussion

As described in the Introduction, there is much evidence indicating that many different peripheral membrane proteins as well as some integral membrane proteins interact with the cytoplasmic face of the plasma membrane via lysine-rich clusters (references 1-10). The present study was conducted to investigate whether cholesterol can modify this interaction.

It was shown that a static light scattering (SLS) increase is only possible in the presence of DOPS, as the addition of PLL to net-neutral vesicles of cholesterol and DOPC did not increase SLS (Figure 1). This showed that DOPS is necessary for an electrostatic interaction to occur with PLL, resulting in vesicle aggregation and enhanced light scattering. This is in agreement with previous light scattering experiments [10] which demonstrated SLS increases only when the added polyamino acid was positively charged (i.e. poly-L-arginine also caused an increase, but poly-L-glutamic acid didn't) and only when the membrane contained negatively charged lipids (i.e. phosphatidylglycerol and phosphatidic acid headgroups also caused PLL-induced SLS increases, but net neutral phosphatidylethanolamine didn't. As a change in SLS or DLS was found to be dependent on the presence of DOPS (i.e. no change is seen for vesicles containing DOPC and cholesterol alone), this indicates that any effect of cholesterol on electrostatic interactions of PLL with vesicles must be indirect *via* DOPS. It is well known that cholesterol increases the density of lipid packing [16, 21, 22, 26, 46]. This increase in DOPS packing would be expected to increase the negative charge density of the membrane, resulting in greater PLL attraction and vesicle aggregation. Furthermore, for 18% DOPS vesicles, DLS showed greater aggregation in the presence of cholesterol than in its

absence, implying cholesterol increases electrostatic interactions between positive lysine residues and negatively charged phospholipids.

PLL addition to 18% DOPS vesicles elicited greater SLS increases in the absence of cholesterol but DLS measurements indicated greater aggregation in the presence of cholesterol. This apparent inconsistency could be explained by differences in the experimental methods. SLS measures changes in scattered light intensity, which are not determined by changes in aggregate size alone. In contrast, DLS measures the dynamics of fluctuations of light scattering intensity, which, in the absence in any changes in the dispersing medium, are only dependent on the aggregate size via its effect on the aggregate's diffusion coefficient. Furthermore, SLS plateauing prior to R_P thresholds cannot be attributed to maximum vesicle aggregation as DLS measurements showed that Z-avg continued to increase across the entire measured range. This suggests another cause of SLS plateauing. Potentially, some of the differences in SLS obtained from different vesicles could be due to contributions from changes in the refractive index difference between the membrane and the surrounding aqueous solution [47-50]. This is also consistent with the observation that different lipid concentrations were necessary for different vesicles to achieve a similar initial SLS. Thus, due to the complication of changes in membrane refractive index and vesicle size both affecting the SLS signal, one must be careful in the interpretation of SLS changes when comparing vesicles of different composition.

Interestingly, although SLS measurements cannot be used as a sole indicator of vesicle size, it was found that on increasing the DOPS composition of the vesicles from 18% to 30%, both a significant drop in the change in SLS (Figure 1) as well as a much reduced Z-avg (Figure 3) were observed upon PLL addition. These results suggest that, although a negatively charged lipid is required to attract PLL to the membrane, if the negative charge density at the surface becomes too large, it becomes difficult for PLL to neutralise enough of the negatively charged lipid headgroups to induce vesicle aggregation. The fact that a change in SLS could be detected

at all for vesicles containing 30% DOPS suggests that SLS is a more sensitive technique for detecting the presence of a membrane interaction than DLS.

Apart from detecting interaction with the membrane, SLS was found to be useful for elucidating R_P thresholds, suspected to be an indicator of membrane disruption. Interestingly, for 18% DOPS vesicles, continuous PLL titration above R_P thresholds further increased Z-avg. It is suspected this could be a consequence of PLL encouraging membrane fragment re-aggregation. Disappearance of the secondary peak at 355 nm, and the major peak maximum shifting from 1245 nm to 1436 nm over time, supported this hypothesis (Figure 4B). Membrane fragment re-aggregation above R_P thresholds could perhaps explain the continuous decline in SLS, since reaggregation would be expected to result in the formation of un-filled particle volumes, allowing light to pass through membrane fragment aggregates. This would lower SLS efficiency whilst increasing particle diameter (Figure 7).

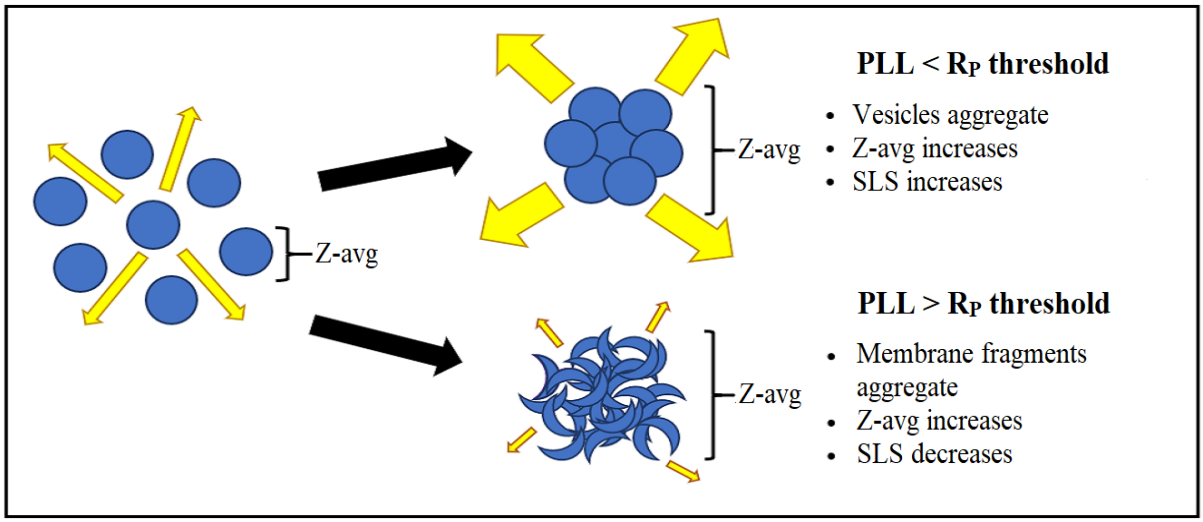

Figure 7: Proposed light scattering effects due to aggregation below and above R_P thresholds.

Similar to measurements on vesicles, the addition of low (<49 μM) and high (≥55 μM) PLL concentrations (given as lysine residue concentrations) to Na^+,K^+-ATPase-containing membrane fragments elicited monophasic and biphasic SLS changes, respectively. This result

suggests that PLL is also able to interact with and penetrate the native membrane environment of the Na^+,K^+-ATPase. This is a significant finding as it strongly indicates that the lysine-rich N-terminus of the protein's α-subunit could insert into the native membrane, which has been suggested as a mechanistic property of Na^+,K^+-ATPase conformation transitions [15, 51].

Carboxyfluorescein (CF) fluorescence intensity changes observed upon maximum PLL addition compared to complete vesicle lysis upon Triton X-100 addition, gave a qualitative measure of PLL penetration, with greater fluorescence intensity increases representative of greater penetration. Importantly, these results clearly showed that PLL is capable of penetrating the membrane. Membrane penetration was also observed for vesicles lacking DOPS (Figure 5). This is in spite of the SLS or DLS measurements, and previous reports [10], failing to identify R_P thresholds or an electrostatic interaction between PLL and DOPC membranes. However, it is important to note that the PLL concentration required to observe lysis of pure DOPC vesicles via CF experiments was much higher that used in the SLS or DLS measurements. For the CF experiments a lysine residue concentration of 303 μM was used, which is an order of magnitude higher than the highest concentration used for SLS and DLS measurements. Thus, together these results would indicate that, although electrostatic interactions with the membrane surface are not an absolute necessity for PLL to penetrate the membrane, electrostatic attraction via negatively charged lipids promote membrane interaction with PLL.

The CF studies clearly demonstrated cholesterol's ability to reduce disruption of neutral membranes by PLL, most likely due to cholesterol condensing phospholipids to increase membrane thickness and mechanical stability. However, CF experiments of DOPS vesicles displayed consistently greater PLL penetration when cholesterol was present. This could be explained by cholesterol's condensing effect of DOPS [16, 21, 22], which would be expected to increase the membrane negative surface charge density, strongly attracting PLL to bind and

penetrate the membrane. Moreover, membrane penetration of cholesterol-containing vesicles was greater when DOPS was present, further suggesting that cholesterol enhanced electrostatic interactions of DOPS to attract PLL and promote membrane penetration relative to neutral vesicles of cholesterol/DOPC. This finding was consistent with DLS measurements, indicating cholesterol increases the electrostatic interaction between the membrane and PLL, as greater vesicle aggregation was seen for DOPS vesicles when cholesterol was present. Furthermore, despite the increased electrostatic interactions, DOPS/cholesterol vesicles underwent lower membrane disruption by PLL than 100% DOPC vesicles, presumably due to the increased packing ability of DOPS and cholesterol's ability to increase membrane thickness and mechanical stability [16, 21, 22].

There was no significant difference in maximum PLL penetration between 18% and 30% DOPS vesicles devoid of cholesterol, but both showed significantly lower levels of penetration than 100% DOPC vesicles. This may indicate that DOPS can cause tighter lipid packing within the membrane, thus providing defence against disruption, despite an increased negative charge to attract PLL. This would seem to support other studies indicating that phosphatidylserine increases membrane thickness and rigidity over phosphatidylcholine bilayers alone [44]. Additionally, cholesterol's effect on the stability of negatively charged membranes displayed a dependence on the relative amounts of negative phospholipid in the membrane, which was postulated to be due to a preference of cholesterol to condense DOPS over DOPC.

In conclusion, the results presented here strongly suggest that the presence of anionic lipids (i.e. DOPS) and increased levels of cholesterol in the membrane dictate the strength of electrostatic interactions between lipid membrane surfaces. Additionally, PLL was found to penetrate the membrane to varying degrees depending on the DOPS and cholesterol membrane compositions. Introduction of either cholesterol or DOPS was found to discourage membrane

penetration relative to 100% DOPC vesicles. Simultaneous introduction of cholesterol and DOPS to the membrane also inhibited PLL penetration of the membrane in comparison to DOPC vesicles. However, the inhibition of PLL's ability to penetrate the membrane was less when both cholesterol and DOPS were included in the membrane than when either cholesterol alone or DOPS alone were included. This suggests that the ability of lysine clusters of membrane proteins to electrostatically interact and penetrate the membrane depends on both the cholesterol and the PS concentration. The complete lysis of the membrane which was observed here at high PLL concentrations, is, however, unlikely to occur in either peripheral or transmembrane proteins, because in these cases the lysine clusters are directly connected through the rest of the polypeptide chain to other protein domains, either in the neighbouring cytoplasm (in the case of peripheral proteins) or embedded in the membrane (in the case of transmembrane proteins).

Acknowledgement

R. J. C. acknowledges financial support from the Australian Research Council (Discovery Grants DP121003548, DP150101112 and DP170101732. F. C. acknowledges financial support of the Danish Medical Research Council and The Novo Nordisk Foundation.

References

[1] D. Murray, A. Arbuzova, B. Honig, S. McLaughlin, The role of electrostatic and nonpolar interactions in the association of peripheral proteins with membranes, Curr. Topics Membr. 52 (2002) 277-307.

[2] C. T. Sigal, W. Zhou, C. A. Buser, S. McLaughlin, M. D. Resh, Amino-terminal basic residues of Src mediate membrane binding through electrostatic interaction with acidic phospholipids, Proc. Natl. Acad. Sci. U. S. A. 91 (1994) 12253-12257.

[3] J. Kim, P. J. Blackshear, J. D. Johnson, S. McLaughlin, Phosphorylation reverses the membrane association of peptides that correspond to the basic domains of MARCKS and neuromodulin, Biophys. J. 67 (1994) 227-237.

[4] J. Kim, T. Shishido, X. Jiang, A. Aderem, S. McLaughlin, Phosphorylation, high ionic strength, and calmodulin reverse the binding of MARCKS to phospholipid vesicles, J. Biol. Chem. 269 (1994) 28214-28219.

[5] M. A. Noguera-Salvà, F. Guardiola-Serrano, M. L. Martin, A. Marcilla-Etxenike, M. O. Bergo, X. Busquets, P. V. Escribá, Role of the C-terminal basic amino acids and the lipid anchor of the $G\gamma_2$ protein in membrane interactions and cell localization, Biochim. Biophys. Acta – Biomembr. 1859 (2017) 1536-1547.

[6] T. J. Maures, H.-W. Su, L. S. Argetsinger, S. Grinstein, C. Carter-Su, Phosphorylation controls a dual-function polybasic nuclear localization sequence in the adapter protein SH2B1β to regulate its cellular function and distribution, J. Cell Sci. 124 (2011) 1542-1552.

[7] F. Lei, J. Jin, C. Herrmann, W. Mothes, Basic residues in the matrix domain and multimerization target murine leukemia virus Gag to the virological synapse, J. Virol. 87 (2013) 7113-7126.

[8] D. Diaz, R.J. Clarke, Evolutionary analysis of the lysine-rich N-terminal cytoplasmic domains of the gastric H^+,K^+-ATPase and the Na^+,K^+-ATPase, J. Membr. Biol. 251 (2018) 653–666. doi:10.1007/s00232-018-0043-x.

[9] C. P. Ptak, L. G. Cuello, E. Perozo, Electrostatic interaction of a K^+ channel RCK domain with charged membrane surfaces, Biochemistry 44 (2005) 62-71.

[10] K. Nguyen, A. Garcia, M.-A. Sani, D. Diaz, V. Dubey, D. Clayton, G. Dal Poggetto, F. Cornelius, R. J. Payne, F. Separovic, H. Khandelia, R. J. Clarke, Interaction of N-terminal peptide analogues of the Na^+,K^+-ATPase with membranes, Biochim. Biophys. Acta – Biomembr. 1860 (2018) 1282-1291.

[11] P. L. Jørgensen, Purification and characterisation of (Na^+,K^+)-ATPase. 5. Conformational-changes in enzyme transitions between Na-form and K-form studied with tryptic digestion as a tool, Biochim. Biophys. Acta 401 (1975) 399-415.

[12] P. L. Jørgensen, E. Skriver, H. Hebert, A. B. Maunsbach, Structure of the Na,K-pump: crystallization of pure membrane-bound Na,K-ATPase and identification of functional domains of the α-subunit, Ann. N. Y. Acad. Sci. 402 (1982) 207-225.

[13] P. L. Jørgensen, J. H.Collins, Tryptic and chymotryptic cleavage sites in sequence of α-subunit of (Na^+ + K^+)-ATPase from outer medulla of mammalian kidney, Biochim.Biophys. Acta 860 (1986) 570-576.

[14] P. L. Jørgensen, J. P. Andersen, Structural basis for E1-E2 conformational transitions in Na,K-pump and Ca-pump proteins, J. Membr. Biol. 103 (1988) 95-120.

[15] Q. Jiang, A. Garcia, M. Han, F. Cornelius, H.J. Apell, H. Khandelia, R.J. Clarke, Electrostatic Stabilization Plays a Central Role in Autoinhibitory Regulation of the Na^+,K^+-ATPase, Biophys. J. 112 (2017) 288–299. doi:10.1016/j.bpj.2016.12.008.

[16] Y.K. Levine, M.H.F. Wilkins, Structure of oriented lipid bilayers, Nat. New Biol. 230 (1971) 69–72. doi:10.1038/newbio230069a0.

[17] P.L. Yeagle, Cholesterol and the cell membrane, BBA - Rev. Biomembr. 822 (1985) 267–287. doi:10.1016/0304-4157(85)90011-5.

[18] D. Needham, R.S. Nunn, Elastic deformation and failure of lipid bilayer membranes containing cholesterol, Biophys. J. 58 (1990) 997–1009. doi:10.1016/S0006-3495(90)82444-9.

[19] F. Schroeder, J.K. Woodford, J. Kavecansky, W.G. Wood, C. Joiner, Cholesterol domains in biological membranes, Mol. Membr. Biol. 12 (1995) 113–119. doi:10.3109/09687689509038505.

[20] S. Raffy, J. Teissié, Control of lipid membrane stability by cholesterol content, Biophys. J. 76 (1999) 2072–2080. doi:10.1016/S0006-3495(99)77363-7.

[21] H. Ohvo-Rekilä, B. Ramstedt, P. Leppimäki, J. Peter Slotte, Cholesterol interactions with phospholipids in membranes, Prog. Lipid Res. 41 (2002) 66–97. doi:10.1016/S0163-7827(01)00020-0.

[22] W.C. Hung, M.T. Lee, F.Y. Chen, H.W. Huang, The condensing effect of cholesterol in lipid bilayers, Biophys. J. 92 (2007) 3960–3967. doi:10.1529/biophysj.106.099234.

[23] F. de Meyer, B. Smit, Effect of cholesterol on the structure of a phospholipid bilayer, Proc. Natl. Acad. Sci. 106 (2009) 3654–3658. doi:10.1073/pnas.0809959106.

[24] J. Grouleff, S.J. Irudayam, K.K. Skeby, B. Schiøtt, The influence of cholesterol on membrane protein structure, function, and dynamics studied by molecular dynamics simulations, Biochim. Biophys. Acta - Biomembr. 1848 (2015) 1783–1795. doi:10.1016/j.bbamem.2015.03.029.

[25] D. Papahadjopoulos, M. Cowden, H. Kimelberg, Role of cholesterol in membranes effects on phospholipid-protein interactions, membrane permeability and enzymatic activity, BBA - Biomembr. 330 (1973) 8–26. doi:10.1016/0005-2736(73)90280-0.

[26] R.A. Demel, J.W.C.M. Jansen, P.W.M. van Dijck, L.L.M. van Deenen, The

preferential interactions of cholesterol with different classes of phospholipids, BBA - Biomembr. 465 (1977) 1–10. doi:10.1016/0005-2736(77)90350-9.

[27] R.A. Cooper, Influence of increased membrane cholesterol on membrane fluidity and cell function in human red blood cells, J. Supramol. Cell. Biochem. 8 (1978) 413–30. doi:10.1002/jss.400080404.

[28] S. Subramaniam, H.M. McConnell, Critical mixing in monolayer mixtures of phospholipid and cholesterol, J. Phys. Chem. 91 (1987) 1715–1718. doi:10.1021/j100291a010.

[29] I. Klodos, M. Esmann, R.L. Post, Large-scale preparation of sodium-potassium ATPase from kidney outer medulla, Kidney Int. 62 (2002) 2097–2100. doi:10.1046/j.1523-1755.2002.00654.x.

[30] P. Ottolenghi, The reversible delipidation of a solubilized sodium-plus-potassium ion-dependent adenosine triphosphatase from the salt gland of the spiny dogfish, Biochem. J. 151 (1975) 61–66. doi:10.1042/bj1510061.

[31] G.L. Peterson, A simplification of the protein assay method of Lowry et al. which is more generally applicable, Anal. Biochem. 83 (1977) 346–356. doi:10.1016/0003-2697(77)90043-4.

[32] O.H. Lowry, N.J. Rosebrough, A.L. Farr, R.J. Randall, Protein measurement with the Folin phenol reagent., J. Biol. Chem. 193 (1951) 265–275. doi:10.1016/0304-3894(92)87011-4.

[33] Brown W, Dynamic Light Scattering: The Method and Some Applications, Clarendon Press, Michigan, 1993. doi:10.1016/S1359-0294(97)80032-5.

[34] J.J.H.H.M. De Pont, A. Van Prooijen-Van Eeden, S.L. Bonting, Role of negatively charged phospholipids in highly purified ($Na^+ + K^+$)-ATPase from rabbit kidney outer medulla. Studies on ($Na^+ + K^+$)-activated ATPase, XXXIX, Biochim. Biophys. Acta -

Biomembr. 508 (1978) 464–477. doi:10.1016/0005-2736(78)90092-5.

[35] W.H.M. Peters, A.M.M. Fleuren-Jakobs, J.J.H.H.M. De Pont, S.L. Bonting, Studies on ($Na^+ + K^+$)-activated ATPase XLIX. Content and role of cholesterol and other neutral lipids in highly purified rabbit kidney enzyme preparation, Biochim. Biophys. Acta - Biomembr. 649 (1981) 541–549. doi:10.1016/0005-2736(81)90158-9.

[36] M. Edidin, Lipids on the frontier: A century of cell-membrane bilayers, Nat. Rev. Mol. Cell Biol. 4 (2003) 414–418. doi:10.1038/nrm1102.

[37] G. Van Meer, D.R. Voelker, G.W. Feigenson, Membrane lipids: Where they are and how they behave, Nat. Rev. Mol. Cell Biol. 9 (2008) 112–124. doi:10.1038/nrm2330.

[38] V.A. Fadok, A. De Cathelineau, D.L. Daleke, P.M. Henson, D.L. Bratton, Loss of phospholipid asymmetry and surface exposure of phosphatidylserine is required for phagocytosis of apoptotic cells by macrophages and fibroblasts, J. Biol. Chem. 276 (2001) 1071–1077. doi:10.1074/jbc.M003649200.

[39] H.M. Hankins, R.D. Baldridge, P. Xu, T.R. Graham, Role of Flippases, Scramblases and Transfer Proteins in Phosphatidylserine Subcellular Distribution, Traffic. 16 (2015) 35–47. doi:10.1111/tra.12233.

[40] M. Reuter, C. Schwieger, A. Meister, G. Karlsson, A. Blume, Poly-l-lysines and poly-l-arginines induce leakage of negatively charged phospholipid vesicles and translocate through the lipid bilayer upon electrostatic binding to the membrane, Biophys. Chem. 144 (2009) 27–37. doi:10.1016/j.bpc.2009.06.002.

[41] D. Volodkin, H. Mohwald, J.C. Voegel, V. Ball, Coating of negatively charged liposomes by polylysine: Drug release study, J. Control. Release. 117 (2007) 111–120. doi:10.1016/j.jconrel.2006.10.021.

[42] D. Volodkin, V. Ball, P. Schaaf, J.C. Voegel, H. Mohwald, Complexation of phosphocholine liposomes with polylysine. Stabilization by surface coverage versus

aggregation, Biochim. Biophys. Acta - Biomembr. 1768 (2007) 280–290. doi:10.1016/j.bbamem.2006.09.015.

[43] R.F. Chen, J.R. Knutson, Mechanism of fluorescence concentration quenching of carboxyfluorescein in liposomes: Energy transfer to nonfluorescent dimers, Anal. Biochem. 172 (1988) 61–77. doi:10.1016/0003-2697(88)90412-5.

[44] H.I. Petrache, S. Tristram-Nagle, K. Gawrisch, D. Harries, V.A. Parsegian, J.F. Nagle, Structure and Fluctuations of Charged Phosphatidylserine Bilayers in the Absence of Salt, Biophys. J. 86 (2004) 1574–1586. doi:10.1016/S0006-3495(04)74225-3.

[45] T.P.W. McMullen, R.N.A.H. Lewis, R.N. McElhaney, Differential scanning calorimetric and fourier transform infrared spectroscopic studies of the effects of cholesterol on the thermotropic phase behavior and organization of a homologous series of linear saturated phosphatidylserine bilayer membranes, Biophys. J. 79 (2000) 2056–2065. doi:10.1016/S0006-3495(00)76453-8.

[46] M.C. Phillips, The Physical State of Phospholipids and Cholesterol in Monolayers, Bilayers, and Membranes, Prog. Surf. Membr. Sci. 5 (1972) 139–221. doi:10.1016/B978-0-12-571805-9.50009-9.

[47] D. Ducharme, J.J. Max, C. Salesse, R.M. Leblanc, Ellipsometric study of the physical states of phosphatidylcholines at the air-water interface, J. Phys. Chem. 94 (1990) 1925–1932. doi:10.1021/j100368a038.

[48] J.G. Petrov, T. Pfohl, H. Möhwald, Ellipsometric Chain Length Dependence of Fatty Acid Langmuir Monolayers. A Heads-and-Tails Model, J. Phys. Chem. B. 103 (1999). doi:10.1021/jp984393o.

[49] R. Horváth, G. Fricsovszky, E. Papp, Application of the optical waveguide lightmode spectroscopy to monitor lipid bilayer phase transition, Biosens. Bioelectron. 18 (2003) 415–428. doi:10.1016/S0956-5663(02)00154-9.

[50] M.C. Howland, A.W. Szmodis, B. Sanii, A.N. Parikh, Characterization of physical properties of supported phospholipid membranes using imaging ellipsometry at optical wavelengths, Biophys. J. 92 (2007) 1306–1317. doi:10.1529/biophysj.106.097071.

[51] A. Garcia, P.R. Pratap, C. Lüpfert, F. Cornelius, D. Jacquemin, B. Lev, T.W. Allen, R.J. Clarke, The voltage-sensitive dye RH421 detects a Na^+,K^+-ATPase conformational change at the membrane surface, Biochim. Biophys. Acta - Biomembr. 1859 (2017) 813–823. doi:10.1016/j.bbamem.2017.01.022.